Angular dependence of magnetization switching for a multidomain dot: Experiment and simulation

O. Fruchart,* J.-C. Toussaint, P.-O. Jubert,† and W. Wernsdorfer
Laboratoire Louis Néel, CNRS, BP166, F-38042 Grenoble Cedex 9, France

R. Hertel and J. Kirschner
Max Plank Institut für Mikrostrukturphysik, D-06120, Halle, Germany

D. Mailly
Laboratoire de Photonique et de Nanostructures, CNRS, Route de Nozay, F-91460 Marcoussis, France
(Received 1 June 2004; published 17 November 2004)

We have measured the in-plane angular variation of nucleation and annihilation fields of a multidomain magnetic single dot with a micro-SQUID. The dots are Fe/Mo(110) self-assembled in ultrahigh vacuum, with submicron size and an elongated hexagonal shape. The angular variations were quantitatively reproduced by micromagnetic simulations. Discontinuities in the variations are observed, and shown to result from bifurcations related to the interplay of the nonuniform magnetization state with the shape of the dot.

DOI: 10.1103/PhysRevB.70.172409 PACS number(s): 75.60.Jk, 75.75.+a, 75.60.Ch

Coherent rotation of magnetization is the simplest model of magnetization reversal, proposed by Stoner and Wohlfarth in 1948.[1] Coherent rotation predicts the value of the switching field H_{swi} of a single-domain system as a function of the direction of the external field H_{ext}. For a two-dimensional system with uniaxial anisotropy the polar plot $H_{\mathrm{swi}}(\varphi)$ falls on the well-known astroid.[2] The full experimental proof for coherent rotation was given only recently, when nanoparticles of high quality and of size small enough to roughly satisfy the hypothesis of uniform magnetization could be investigated individually.[3,4] Starting from this proof, it is now a challenge to understand magnetization reversal in increasingly large (and thus complex) systems. The simplest ingredient to add to coherent rotation is to allow minor deviations from strictly homogeneous magnetization. The consequences on magnetization processes were addressed by numerical micromagnetics,[5] investigated analytically[6] and checked experimentally.[7] The next step is now to tackle quantitatively more strongly non-uniform systems, those that may display magnetic domains and domain walls.[8] In such systems a switching field H_{swi} is not the signature of the full reversal of magnetization, but instead reflects events like nucleation, propagation and annihilation.[9] Few and only partial experimental[9] and numerical[10] reports are found on this issue. A more detailed study would open the door to understanding microscopic details of magnetization reversal processes in macroscopic materials. In this Report we present such a study in a model system: sub-micrometer-sized Fe faceted dots self-assembled in UHV, that have a high structural quality and display simple multidomain states.[11,12] The angular dependence of the H_{swi}'s of a single dot was studied with the micro-SQUID technique.[13] This can be seen as the first experimental generalization of astroids for an individual multidomain system. A striking feature is the occurrence of discontinuities (hereafter named jumps) in $H_{\mathrm{swi}}(\varphi)$ plots. These jumps were reproduced and understood with the help of numerical micromagnetism. They result from bifurcations, related to the interplay of the nonuniform magnetization with the shape of the dot. This also shows that a complex H_{swi} behavior does not necessarily result from defects.

The Fe(110) epitaxial dots were fabricated with pulsed laser deposition in ultrahigh vacuum by self-assembly on Mo(110)[8 nm]/$Al_2O_3(11\bar{2}0)$. The dots display the shape of ingots with atomically flat facets, bulk lattice parameter and bulk cubic magnetocrystalline anisotropy K_1 favoring $\langle 100\rangle$ axes, however of magnitude much smaller than $\frac{1}{2}\mu_0 M_s^2$.[11] The interdot dipolar fields are negligible with respect to H_{swi}. The remanent state consists of flux-closure domains, resulting from demagnetizing fields within each dot.[12] Such domains can occur due to the size of the dots being well above the exchange length Λ_{ex}.[14,15] The in-plane H_{swi}'s of a single Fe dot were measured below 4 K using the micro-SQUID technique.[13] For these measurements, the dots were covered in UHV by Mo[2 nm], followed by Al[2 nm](then 12 hours air-oxidized), and a Si[2 nm]\Nb[15 nm]\Si[2 nm] trilayer. Arrays of square micro-SQUIDs with edge 1×1 μm were patterned by *e*-beam lithography and SF_6 reactive ion etching of the trilayer. The oxidized Al layer prevents ferromagnetic-superconductor proximity effects between the dots and the micro-SQUIDs. Although the dots are randomly distributed on the surface, their large number yields a significant probability to find one dot suitably coupled to a micro-SQUID. The location and shape of the single dots under investigation were checked *a posteriori* by AFM. The size of the dot selected here [Fig. 1(a)] is $420\times 200\times 30$ nm [Fig. 1(b)]. Micromagnetic simulations were performed for 0 K (no thermal activation) using custom-developed codes, either based on integrating the LLG equation in a finite differences code (rectangular prisms)[16] or on energy minimization in a finite elements code (tetrahedra).[17] The applied field was increased stepwise in hysteresis loops. In finite differences the sample was divided into cells with uniform lateral and vertical size $\Delta_x=\Delta_y=4.70$ nm and $\Delta_z=3.75$ nm, respectively. For

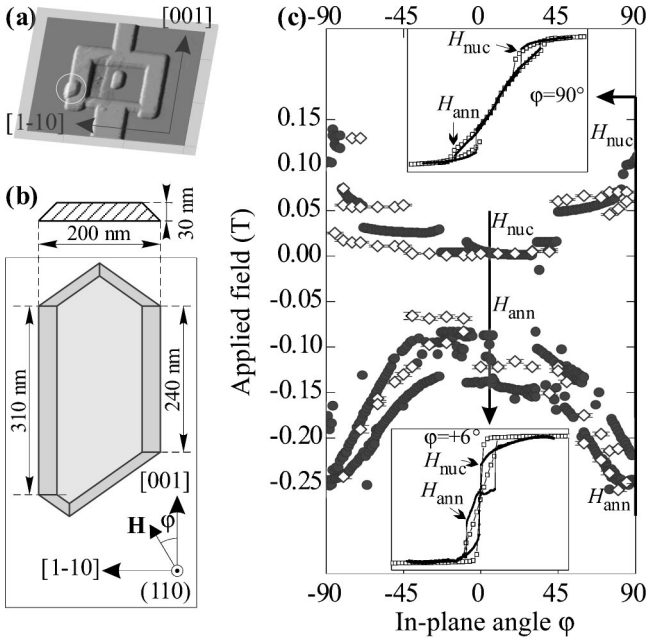

FIG. 1. (a) AFM picture of the micro-SQUID. The dot strongly coupled to the micro-SQUID is indicated by a circle. (b) Top view of the dot. (c) Plot of H_{nuc} (positive) and H_{ann} (negative) for experiments (full symbols) and simulations (open symbols). Insets, experimental and simulated loops for two angles.

finite elements 83 310 tetrahedra of irregular but similar shape were used, with a maximum (respectively, minimum) volume of 42.29 nm^3 (respectively, 12.50 nm^3). We set $K_1=4.8\times10^4$ J m^{-3}, $A=2\times10^{-11}$ J m^{-1}, and $M_s=1.73\times10^6$ A m^{-1} in the calculation.

In the following we call φ the angle between the in-plane H_{ext} and the in-plane long axis of the dot [001] [Fig. 1(b)]. Due to a shape effect, in-plane $[1\bar{1}0]$ ($\varphi=90°$) is a magnetically harder direction than [001]. The insets of Fig. 1(c) show micro-SQUID hysteresis loops for two angles ($\varphi=+6;+90°$). Such loops with negligible remanence although with significant hysteresis, are characteristic of multidomain systems with a limited number of domains. Starting from positive saturation the first H_{swi}, named hereafter H_{nuc}, is expected to reveal a *nucleation* event, e.g., the entry of a magnetic vortex[18] in the dot. The second H_{swi}, occurring at negative fields and named H_{ann}, is expected to reveal an *annihilation* event, i.e., the expulsion from the dot of a previously nucleated vortex or wall. Figure 1(c) shows the experimental angular variation of $H_{nuc}(\varphi)$ and $H_{ann}(\varphi)$. The twofold symmetry results from the elongated shape of the dot. Two striking features are observed, that shall be explained in the course of the discussion. First, jumps of both H_{nuc} and H_{ann} occur at some angles. Second, depending on the range of angles, one or two H_{nuc} and/or H_{ann} are observed. Notice that statistical measurements were performed for a small number of φ values, which showed that fluctuations in H_{swi} values from one loop to another are much smaller than separation between successive H_{swi} in a loop, or than $H_{swi}(\varphi)$ jumps.

The jumps of H_{swi} can be understood qualitatively by simple arguments. Let us sketch in a quasistatic picture the

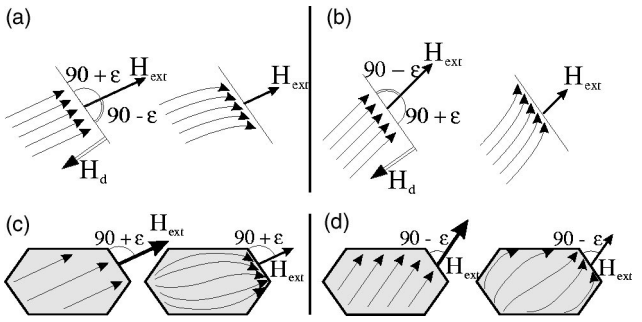

FIG. 2. Schematic illustration of magnetization state bifurcation related to the orientation of the external field H_{ext} with respect to an edge. The length of arrows sketches the magnitude of H_{ext}. The external field H_{ext} is tilted (a) clockwise or (b) anticlockwise with respect to the normal to the edge. For a hexagonal dot, just after bifurcation the magnetization state may thus be in a leaf state (Ref. 6) oriented either along the (c) long edge or (d) diagonal.

evolution of magnetization $\mathbf{M}(\mathbf{r})$ close to an edge during the first stages of a hysteresis loop [Figs. 2(a) and 2(b)]. Starting from saturation, upon decrease of H_{ext} the *relative* importance of the dipolar energy E_d increases. As a result $\mathbf{M}$ progressively rotates towards the edge to reduce surface charges, and thus reduce E_d. The direction of rotation, clockwise or anticlockwise, depends on the initial direction of $\mathbf{M}$ with respect to the normal to the edge (imposed by the direction of H_{ext}), due to the torque exerted by the dipolar field H_d on $\mathbf{M}$. With this picture at least two different slightly inhomogeneous magnetization states, so-called "leaf states,"[6] are expected to appear upon decrease of H_{ext}, e.g., when starting from saturation along $\varphi=0°$ or $\varphi=90°$ [Figs. 2(c) and 2(d)]. Bifurcation must occur for at least one intermediate angle between these two paths. Then, it is obvious that for H_{ext} applied on either side of this angle, the magnetization pattern will evolve towards very different states, each characterized by a different entry point for vortices—and thus of edge orientation, explaining a jump in $H_{nuc}(\varphi)$. These ideas were confirmed by micromagnetic simulation. In a first attempt the simulations were performed on a dot with vertical facets and symmetric ends. Figures 3(a) and 3(b) show the static magnetization states just before and after H_{nuc}. For $\varphi=40°$, before H_{nuc} the state belongs to the class sketched in Fig. 2(c), as expected. Then two regions of strongly nonuniform magnetization develop simultaneously, ending up in the entry of two vortices at H_{nuc}. As H_{ext} is further decreased the two vortices with opposite circulation move towards the inner part of the dot, ending up in a diamond state [Fig. 3(a)]. For $\varphi=50°$ the state before nucleation looks like that in Fig. 2(d). The loci of the entering vortices are thus modified with respect to the above situation, explaining the jump of H_{nuc}, but ending as well in a diamond state, i.e., with two vortices [Fig. 3(b)].

The above arguments explain the jumps of H_{nuc}, but fail to explain (1) the existence of either one or two H_{nuc} and H_{ann} for some angles [Fig. 1(c)], (2) the experimental observation of both diamond and Landau states,[12] i.e., with two or one wall or vortex. Indeed in the simulations for any φ two vortices appear simultaneously at opposite loci, as the dot was assumed to be perfectly symmetric. Due to the large dot

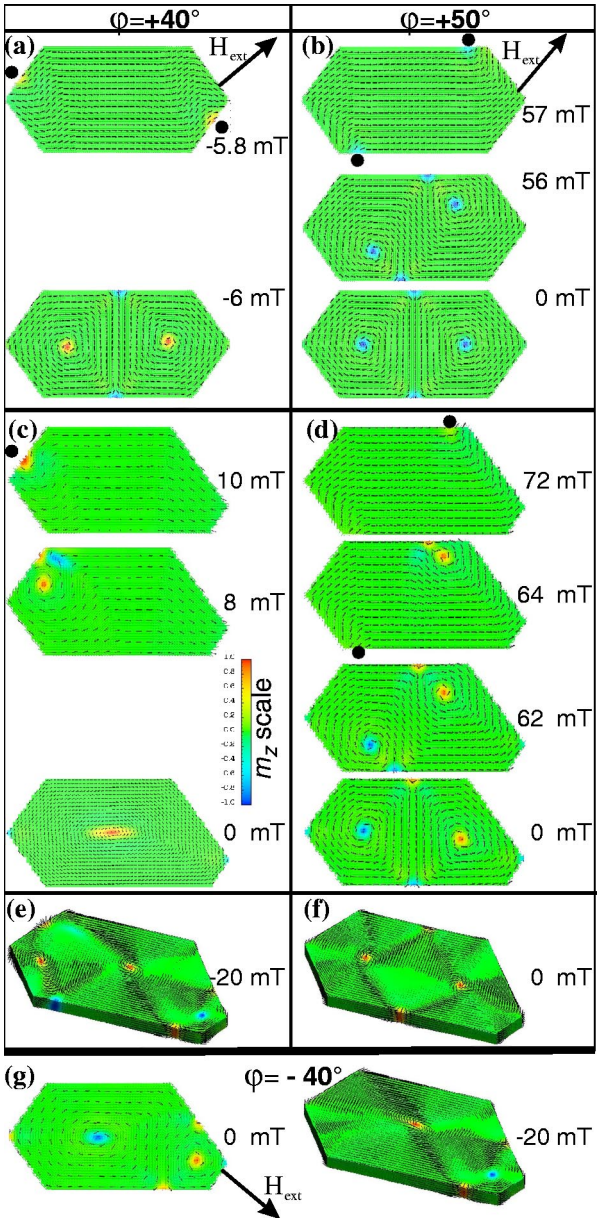

FIG. 3. (a)–(d) Mid-height views of micromagnetic finite differences simulations of dots with vertical facets, for $\varphi=40°$ (left) and $\varphi=50°$ (right), for (a) and (b) symmetric and (c) and (d) asymmetric in-plane shape. H_{ext} is decreased from positive saturation towards the flux-closure state. Nucleation loci are indicated with full dots. (e) and (f) Flux-closure state obtained on the same element with finite elements simulations (surface views). (g) Flux-closure states for $\varphi=-40°$, for finite differences (left) and finite elements (right). The shading codes the perpendicular component of magnetization (see scale). Notice that the remanent state is displayed only for those cases where the nucleation field is positive.

size these vortices interact weakly with each other, thus both enter the dot, ending up in a diamond state. In order to refine our interpretations, we now report simulations performed on dots with a slightly asymmetric shape, similar to that of the AFM observation of the measured dot [Fig. 1(a)]. Opposite loci are no more equivalent due to the point-reversal symmetry breaking. Two situations occur. If opposite loci are similar then two vortices still enter the dot, one slightly before the other in terms of H_{ext}, however still ending in the diamond state [e.g., for $\varphi=+50°$, Fig. 3(d)]. If opposite loci are significantly different, then one of the vortices may enter the dot at a much higher field than the other. It then moves towards its center, delaying and possibly preventing the entry of a second main vortex. This ends up in a Landau state [e.g., for $\varphi=+40°$, Fig. 3(c)]. Notice that the vortex may continuously change its shape into a Bloch wall, provided that the dot is long and thick enough.[12,19] Thus, an asymmetric feature (like shape) is necessary to explain the experimental observation of one-wall/vortex state.[12] Notice also that sometimes more than two vortices may appear [Figs. 3(e)–3(g)]. Figure 1(c) (upper part) shows that these simulations reproduce experimental $H_{nuc}(\varphi)$ convincingly. As a further step some simulations were performed on dots with inclined facets, i.e., as close as possible to the experimental case. This was done in the finite-element scheme to avoid numerical roughness on the surfaces.[20] This yielded results quantitatively similar to the case of vertical facets.

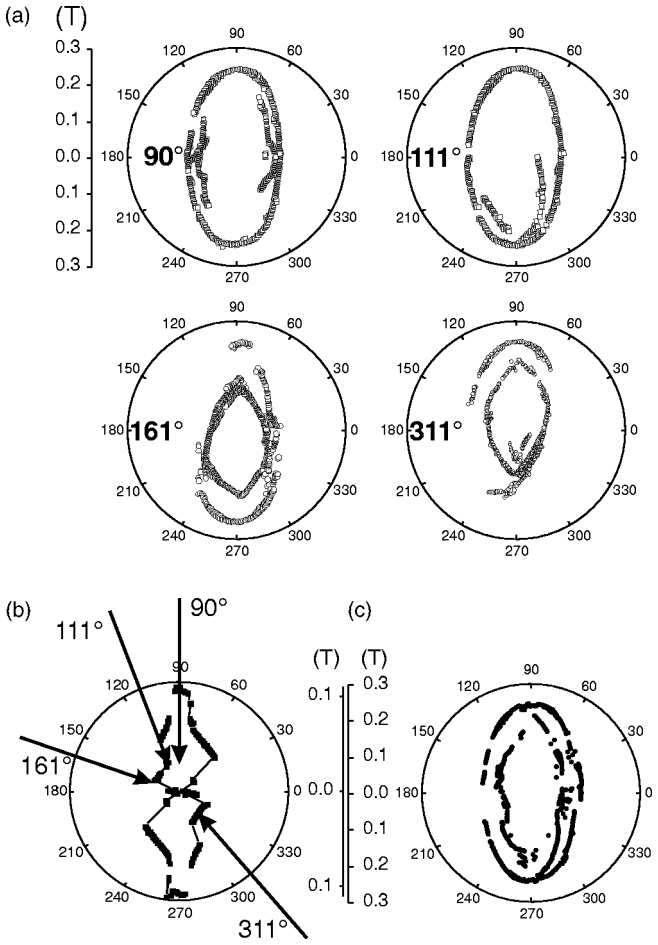

FIG. 4. (a) Polar plots $H_{ann}(\varphi_2)$ starting from different zero-field states, each state being prepared by initial saturation along a given direction φ_1, shown in (b) with respect to the $H_{nuc}(\varphi)$ plot. (c) Polar plot of $H_{ann}(\varphi)$ for radial field sweeping (same data as Fig. 1(c)).

Simulations of $H_{ann}(\varphi)$ [lower part of Fig. 1(c)] also reproduce experimental data. The jumps of $H_{ann}(\varphi)$ again result from the bifurcation before nucleation, implying differ-

ent states before annihilation. The occurrence of one versus two H_{ann} may be associated with the occurrence of different flux-closure states at low field. A more general experiment consists in proceeding to nucleation with the field decreased along a given angle φ_1, followed by annihilation with the field increased along a different direction φ_2. The plot $H_{ann}(\varphi_2)$, measured while keeping φ_1 fixed, i.e., trying to prepare the system always in the same remanent state as a starting point, can be viewed as a signature of this state. Figure 4(a) displays such plots for several values of φ_1, chosen in different branches of the experimental H_{nuc} [Fig. 4(b)]. The plots are not identical, which confirms that the remanent state depends on the angle of H_{ext}. The fact that different plots roughly consist of different parts of a common set of two branches is also easily understood. For a given φ_2 a wall or a vortex of given circulation will always be pushed towards the same locus of the dot, be it alone at remanence (vortex or Landau state) or having a companion (diamond state). In the latter case one point is found on each branch, whereas in the former case only one branch is revealed.

Finally, the values of H_{swi} depend only weakly on the algorithm used (finite differences or finite elements). However, sometimes fine differences appear upon nucleation, such as the magnetization direction of vortices' cores or surface head-to-head or tail-to-tail structures on the vertical side facets, or the occurrence of more than two vortices [see Figs. 3, (c) vs (e), (d) vs (f), (g)], although both codes were benchmarked successfully one against each other on time-resolved magnetization reversal issues.[21] This underlines that describing the fine details of nucleation with simulations remains a challenge and that results should still be taken with care.

To conclude, we reported the measurements, quantitative reproduction, and understanding of angular nucleation and annihilation fields $H_{nuc}(\varphi)$ and $H_{ann}(\varphi)$ in a multidomain magnetic particle. This is an example of a generalization to multidomain states of the well-known Stoner-Wohlfarth astroid. The main feature is the occurrence of jumps in both plots, which result from the interplay of a nonuniform magnetization state with the shape of the dot. Thus, such jumps should not be automatically ascribed to defects when observed in experiments.

The authors thank Ph. David and V. Santonacci for technical support, and C. Meyer for critically reading the paper.

*Electronic address: olivier.fruchart@grenoble.cnrs.fr
†Present address: IBM Research - Zurich Research Laboratory, 8803 Rüschlikon, Switzerland.

[1] E. C. Stoner and E. P. Wohlfarth, Philos. Trans. R. Soc. London, Ser. A **240**, 599 (1948).
[2] J. C. Slonczewski, Research Memo RM 003.111.224, IBM Research Center, Poughkeepsie, NY.
[3] W. Wernsdorfer, E. Bonet-Orozco, K. Hasselbach, A. Benoit, B. Barbara, N. Demoncy, A. Loiseau, H. Pascard, and D. Mailly, Phys. Rev. Lett. **78**, 1791 (1997).
[4] E. Bonet-Orozco, W. Wernsdorfer, B. Barbara, A. Benoit, D. Mailly, and A. Thiaville, Phys. Rev. Lett. **83**, 4188 (1999).
[5] M. A. Schabes and H. N. Bertram, J. Appl. Phys. **64**, 1347 (1988).
[6] R. P. Cowburn and M. E. Welland, Phys. Rev. B **58**, 9217 (1998).
[7] R. P. Cowburn, A. O. Adeyeye, and M. E. Welland, Phys. Rev. Lett. **81**, 5414 (1998).
[8] A. Hubert and R. Schäfer, *Magnetic Domains. The Analysis of Magnetic Microstructures* (Springer, Berlin, 1999).
[9] W. Wernsdorfer, K. Hasselbach, A. Sulpice, A. Benoit, J.-E. Wegrowe, L. Thomas, B. Barbara, and D. Mailly, Phys. Rev. B **53**, 3341 (1996).
[10] Z. H. Wei, C. R. Chang, N. A. Usov, M. F. Lai, and J. C. Wu, J. Magn. Magn. Mater. **239**, 1 (2002).
[11] P.-O. Jubert, O. Fruchart, and C. Meyer, Phys. Rev. B **64**, 115419 (2001).
[12] P. O. Jubert, J. C. Toussaint, O. Fruchart, C. Meyer, and Y. Samson, Europhys. Lett. **63**, 135 (2003).
[13] W. Wernsdorfer, in *Advances in Chemical Physics*, edited by I. Prigogine and S. A. Rice (Wiley, New York, 2001), Vol. 118.
[14] E. H. Frei, S. Shtrikman, and D. Treves, Phys. Rev. **106**, 446 (1957).
[15] H. Kronmüller, Z. Phys. **168**, 478 (1962).
[16] J. C. Toussaint, A. Marty, N. Vukadinovic, J. Ben Youssef, and M. Labrune, Comput. Mater. Sci. **24**, 175 (2002).
[17] R. Hertel, J. Appl. Phys. **90**, 5752 (2001).
[18] K. Y. Guslienko and K. L. Metlov, Phys. Rev. B **63**, 100403(R) (2001).
[19] R. Hertel and H. Kronmüller, Phys. Rev. B **60**, 7366 (1999).
[20] C. J. García-Cervera, Z. Gimbutas, and E. Weinan, J. Comput. Phys. **184**, 37 (2003).
[21] NIST standard problem 4, see http://www.ctcms.nist.gov/mumag/mumag.org.html